

Deconfinement, Center Symmetry and the Ghost Propagator in Landau Gauge Pure SU(3) Yang-Mills Theory

Vítor Paiva,^{*} Paulo J. Silva,[†] and Orlando Oliveira[‡]

CFisUC, Department of Physics, University of Coimbra, 3004-516 Coimbra, Portugal

(Dated: July 18, 2023)

The temperature dependence of the Landau gauge ghost propagator is investigated in pure SU(3) Yang-Mills theory with lattice QCD simulations. Its behavior around the confined-deconfined phase transition temperature, $T_c \sim 270$ MeV, is investigated. The simulations show that in the deconfined phase, the ghost propagator is enhanced for small momenta, $\lesssim 1$ GeV. Furthermore, the analysis of the spontaneous breaking of center symmetry on the ghost propagator is studied. Similarly as observed for the gluon propagator, the simulations result in a decoupling of the sectors where the phase of the Polyakov loop is either 0 or $\pm 2\pi/3$ sectors, with the latter remaining indistinguishable. The results point to the possible use of the ghost propagator as an "order parameter" for the confined-deconfined phase transition.

Contents

I. Introduction and Motivation	1
II. Lattice Setup and the Landau Gauge Ghost Propagator	3
III. Ghost Propagator — Temperature effects	3
IV. Ghost Propagator and center symmetry	4
V. Summary and Conclusions	5
Acknowledgements	6
References	6

I. INTRODUCTION AND MOTIVATION

The dynamics of quarks and gluons feels the effects of the surrounding hadronic environment that translates into a rich QCD phase diagram, see e.g. [1–3] and citations therein. The QCD phase diagram is accessed through the Green functions and, therefore, the fundamental propagators and vertices are not blind to temperature T , density ρ , external magnetic fields or any other field felt by the fundamental QCD quanta. For example, at zero hadronic density, from the quark propagator one can compute the running quark mass that shows different patterns at low and high temperatures. At zero and low temperatures the running quark mass is momentum independent, illustrating the chiral symmetry breaking mechanism [4, 5]. On the other hand, for sufficiently high temperatures, (quenched) lattice results for the quark propagator suggest that chiral symmetry is restored and that

quarks behave essentially as free particles [6]. These results suggest that as the hadronic temperature increases, quarks go from a confined phase, where they appear as constituents of hadrons, to a deconfined phase with the formation of a strongly interacting plasma of quarks and gluons. Moreover, the studies of the finite temperature gluon propagator also show an equivalent transition for the same range of temperatures — see, for example, [15]. This change implies a modification of the analytical properties of the propagator that has been foreseen by several studies.

For full QCD, the temperature where the transition between phases occurs has been estimated to be $T_c \sim 150$ MeV [7, 8]. The investigation of full QCD is demanding and, alternatively, the study of pure Yang-Mills theory, which is less complex due to the dismissal of quark contributions to the dynamics, can help understand the behavior of hadronic matter at finite temperature. The main differences with respect to full QCD are the nature of the order of the phase transition and that gluons become deconfined at higher temperatures. For pure SU(3) Yang-Mills the confined-deconfined transition is first order and the critical temperature is $T_c \sim 270$ MeV.

For pure SU(3) Yang-Mills theory, the transition from low temperatures to higher temperatures can be observed by looking at the gluon propagator, see e.g. [9, 11–18, 50] and references therein. At zero temperature the gluon propagator in the minimal Landau gauge is finite for all range of momenta. The theory generates dynamically a mass scale, and the propagator exhibits positivity violation that can be viewed as an indication of gluon confinement [19–21]. At finite temperature the gluon propagator has an electric and a magnetic form factor, and it is common to associate a mass scale with each component. For temperatures above T_c , these electric and magnetic masses scale differently with temperature [22]. From the point of view of the confined-to-deconfined phase transition, it was observed that the electric form factor can be used to identify the transition and its nature [15, 23, 50]. Moreover, for sufficiently high temperatures the gluons behave as quasi-particles with a finite mass that grows with T . The behaviour of the ghost propagator below

^{*}Electronic address: vpaiva462@gmail.com

[†]Electronic address: psilva@uc.pt

[‡]Electronic address: orlando@uc.pt

and above T_c has been touched in [14], with the lattice QCD results suggesting an enhancement of the IR propagator that grows with T , but a systematic study and specially the role of the center symmetry is still missing in the literature. The current work aims to fill this gap and investigate these issues close to the critical temperature associated with the confined-to-deconfined transition.

In QCD, like in any gauge theory, the set of gauge related configurations, i.e. the configurations on a gauge orbit, are equivalent and express the same physical content. Choosing a gauge means identifying a gauge configuration on each gauge orbit. This represents a problem not yet solved in the quantization of Yang-Mills theories. Despite the gauge fixing procedure being fundamental to handle gauge fields, given the complexity involved, in this paper we will not discuss the issues related to choice of a gauge. We just recall the reader that how gauge fixing is implemented can impact on the IR propagators [25–29].

For pure Yang-Mills SU(N) theory the order parameter for the confined-to-deconfined transition is the Polyakov loop that in the continuum formulation and in Euclidean space-time is defined as

$$L(\vec{x}) = \frac{1}{N} \text{Tr} \left\{ \mathcal{P} \exp \left[i g \int_0^{1/T} dx_4 A_4(\vec{x}, x_4) \right] \right\}, \quad (1)$$

where \mathcal{P} means path ordering and T is the temperature. The space average of the Polyakov loop

$$L = \langle L(\vec{x}) \rangle_{\vec{x}} \propto e^{-F_q/T} \quad (2)$$

measures the free energy of a static quark F_q , see e.g. [22]. In the confined phase where $T < T_c$ the quark free energy is infinite and it follows that the renormalized Polyakov loop is $L = 0$. For temperatures above T_c the renormalized space averaged Polyakov loop is one [24]; it follows that $F_q = 0$, meaning that quarks behave essentially as free particles. The Polyakov loop is associated with the gluon content of the theory. On a finite hypercubic $N_x^3 \times N_t$ lattice the bare Polyakov loop is given by

$$L(\vec{x}) = \prod_{x_4=0}^{N_t} \mathcal{U}_4(\vec{x}, x_4) \quad (3)$$

where \mathcal{U}_4 is the time-oriented link.

For pure Yang-Mills theory the generating functional and, therefore, the Green functions have an additional symmetry associated with an invariance under global gauge transformations of the center group. For $N = 3$ the center group is

$$Z_3 = \left\{ 1, e^{i2\pi/3}, e^{-i2\pi/3} \right\} \quad (4)$$

and divide the group SU(3) into equivalent classes. A Z_3 global transformation leaves the action unchanged, but the Polyakov loop L acquires an extra phase. Note that this invariance applies for both the continuum and

lattice formulations. The inclusion of fermions breaks the center symmetry and can change the nature of the phase transition, see e.g. [30] and references therein.

Our lattice study for the pure gauge SU(3) Yang-Mills theory uses the Wilson action. To explore the center symmetry and, in particular, the breaking of the center symmetry for $T > T_c$, one considers the transformation where the links on a given hyperplane chosen at $x_4 = \text{const}$ are multiplied by $z \in Z_3$. Under this transformation, the Polyakov loop $L(\vec{x})$ becomes $z L(\vec{x})$. In the confined phase, $L = 0$ and the space averaged Polyakov loop is invariant under center transformations. However, for temperatures above T_c , where $L \neq 0$, the Polyakov loop phase is changed by the center transformation and, in this way, one can go through the various equivalent classes and compute, for each class of gauge configurations, the propagator. In this way one can investigate how the breaking of the center symmetry impacts the fundamental fields.

For the minimal Landau gauge and the SU(3) group, the gluon propagator was studied in [23] below and above the critical temperature. The authors showed that for temperatures below T_c the gluon propagator is the same, within the statistical precision achieved in the simulation, for all the equivalent classes. For $T > T_c$ it was found that the gluon propagator differs, mainly at low momenta, between the class of configurations associated with a vanishing phase of the Polyakov loop, let us call it the zero sector, and the other two sectors where the phase of L is $\pm 2\pi/3$. Then, for temperatures above the critical temperature the center symmetry is spontaneously broken. Moreover, this difference can be used as an order parameter to identify the transition to the deconfined phase.

Herein, we pursue and extend the work of [23] to the ghost sector. The details of the sampling, gauge fixing, of the mapping and identification of each of the equivalent classes of gauge configurations can be read in the above cited paper. The computation of ghost sector requires the inversion of a large sparse matrix and, therefore, it is computationally demanding. For this reason, only a subset of the gauge configurations, for temperatures above and below T_c , considered in [23] will be investigated for each of the equivalent classes. As described below we observe that above T_c , the ghost propagator is enhanced in the infrared region and, as for the gluon propagator, the ghost propagator in the zero sector differs from the ghost propagator in the two equivalent classes where L acquires a non-vanishing phase. Indeed, the low momentum ghost propagator in the zero sector is enhanced when compared to the other equivalent classes. Recall that for the gluon propagator, the transverse (electric) form factor is enhanced in the zero sector, relative to the other equivalent classes, while the longitudinal (magnetic) form factor associated with the zero sector is suppressed relative to the remaining sectors, see [23]. The observed correlation between the ghost and the gluon electric and magnetic form factors remains to be understood theoret-

T (MeV)	β	N_s	N_t	a (fm)	$1/a$ (GeV)
121	6.0000	64	16	0.1016	1.943
194	6.0000	64	10	0.1016	1.943
243	6.0000	64	8	0.1016	1.943
260	6.0347	68	8	0.09502	2.0767
265	5.8876	52	6	0.1243	1.5881
275	6.0684	72	8	0.08974	2.1989
324	6.0000	64	6	0.1016	1.943
366	6.0684	72	6	0.08974	2.1989
486	6.0000	64	4	0.1016	1.943

TABLE I: Lattice setup. Each T uses 100 gauge configurations and, for each inversion to compute the ghost propagator, two point sources were averaged. See main text for details.

ically. As for the gluon propagator, we observe that the differences seen in the ghost propagator computed for the different Z_3 sectors can be used to identify the confined-to-deconfined transition and, therefore, the spontaneous symmetry breaking of the center symmetry. Preliminary results can be found in [31].

The current work is organised as follows. In Sec. II, the lattice setup is outlined, focusing on the procedures set for the statistical analysis of the Monte Carlo simulations, the elimination of lattice artefacts and data renormalization. In Sec. III, the effects of temperature on the ghost propagator are discussed. In Sec. IV, the effects of the spontaneous center symmetry breaking on the ghost propagator are analyzed. Finally, in Sec. V, a summary of the main results and a direction toward future studies are presented.

II. LATTICE SETUP AND THE LANDAU GAUGE GHOST PROPAGATOR

The QCD simulations reported here use lattices $N_s^3 \times N_t$, with $N_t \ll N_s$. The temperature is defined as $T = 1/N_t a$, where a is the lattice spacing. We use the Wilson gauge action to perform the importance sampling. The ghost propagator in momentum space is given by

$$G^{ab}(p) = -\delta^{ab} G(p^2) = -\delta^{ab} \frac{d_g(p^2)}{p^2}, \quad (5)$$

where the latin letters refer to color indices, $G(p^2)$ is the ghost propagator and $d_g(p^2)$ is the ghost dressing function. On the lattice, the inverse of the ghost propagator is given by the second variation of the gauge fixing functional that results on a large sparse matrix. This matrix has zero modes and for the computation of ghost propagator, its inversion is performed using the conjugate gradient method following [32]. All computer simulations have been done with the help of Chroma [52] and PFFT [55] libraries.

The lattice setup used in the investigation of the ghost sector reported in Section III is summarized in Tab. I. For each temperature, 100 gauge configurations rotated

to the Landau gauge were considered and, in the computation of the ghost propagator we used two point sources to compute point-to-all propagators. As point sources we took the lattice origin $(0, 0, 0, 0)$ and the lattice spatial mid-point $(N_s/2, N_s/2, N_s/2, 0)$. The corresponding momentum propagators for the two point sources were averaged, and the average used in the statistical analysis of the Monte Carlo simulation. As in previous works, herein only the results coming from the first Matsubara frequency are reported.

The formulation of the gauge theory on a finite hypercubic lattice breaks rotational symmetry and introduces lattice artefacts. In order to minimise the lattice artefacts, the large momenta, defined as the physical momenta above 1 GeV, were subject of a cylindrical cut [33]. The momenta cut chooses only the momenta whose distance, d , from the lattice diagonal, is such that $da < 4(2\pi/N_s)$, i.e. it considers only momenta less than four spatial units away from the lattice's diagonal, $(p, p, p, 0)$.

In order to be able to compare the results of simulations performed with different lattice spacings, the ghost data has to be renormalized. Herein, the renormalization was performed at $\mu = 4$ GeV, demanding that $G(\mu^2) = 1/\mu^2$. In the computation of the renormalization constants Z , for each simulation the lattice data was fitted to the functional form

$$G_{fit}(p^2) = \frac{b + cp^2}{p^4 + dp^2 + e}, \quad (6)$$

where b , c , d and e are adjustable parameters, and then

$$Z = \frac{1}{\mu^2 G_{fit}(\mu^2)}. \quad (7)$$

The fits were performed for momenta in the range [3, 5] GeV and the associated $\chi^2/d.o.f. \sim 1$.

III. GHOST PROPAGATOR — TEMPERATURE EFFECTS

In this section we report on the dependence of the Landau gauge ghost propagator with temperature. The configurations used are such that the phase of the Polyakov loop vanishes. As described previously, this can be achieved exploring the center symmetry transformations. Moreover, the lattice data is described as a function of the improved lattice momentum

$$q_\mu = \frac{2}{a} \sin\left(\frac{\pi}{N_\mu} n_\mu\right),$$

$$n_\mu = -\frac{N_\mu}{2}, \dots, -1, 0, 1, \dots, \frac{N_\mu}{2} - 1, \quad (8)$$

where N_μ is the number of lattice points in direction μ , a is the lattice spacing, and not as a function of the lattice naive momentum

$$p_\mu = \frac{2\pi}{aN_\mu} n_\mu. \quad (9)$$

The motivation for using q_μ instead of p_μ comes from lattice perturbation theory. Recall that for bosonic fields the propagator is a function of q^2 and not of p^2 , see e.g. [34], and also because it was observed that using q instead of p reduce the lattice artefacts, see [28, 33, 35–38].

The Landau gauge ghost propagator and dressing function for various T can be seen in Fig. 1. As a first comment to the results we notice that the qualitative behavior of the ghost propagator at finite T follows the momentum dependence observed at $T = 0$, see e.g. [39–43] and references therein. In the infrared region, $G(p^2)$ diverges with a power greater than the prediction of perturbation theory as can be observed in the right hand plot of Fig. 1. For zero temperature there are several studies that support a pole at zero momentum for the lattice ghost propagator [16, 44, 45], and the data reported in Fig. 1 suggests that the same should occur for finite T . Furthermore, by fitting the lattice Landau ghost propagator at the highest available momenta, in all cases, the lattice data is well reproduced by the tree level perturbation result for $p \gtrsim 5$ GeV. Indeed, for the fits of the lattice data to

$$G(p^2) = \frac{Z}{p^2} \quad (10)$$

it follows that $\chi^2/d.o.f. \sim 1$ and the corresponding residua are $Z \sim 1$. Certainly, the inclusion of the leading log will improve the range of momenta where the matching between lattice simulations and perturbation theory occurs, see e.g. [46]. We take this result as an indication that, in the ultraviolet region, the lattice data reproduces the prediction of perturbation theory.

The second comment concerns the temperature dependence of $G(p^2)$ or, equivalently, of $d_G(p^2)$. As can be observed in Fig. 1 the ghost propagator at low momenta increases when the temperature is increased. The enhancement of the infrared $G(p^2)$ is stronger when the confinement-to-deconfinement temperature is crossed that for pure Yang-Mills takes the value $T_c \sim 270$ MeV, see [23, 47–49] and references therein. Note that in Fig. 1 the results of the simulations for $T > T_c$ are represented by open symbols. To illustrate the stronger enhancement that occurs around $T \sim T_c$, in Fig. 2 we show the ghost dressing function for the smallest momenta available in each simulation, $q \sim 0.19$ GeV. The curve mimics the behavior observed for the temperature dependence of the longitudinal gluon propagator [23, 50] and suggests that, similarly to the gluon propagator, the ghost propagator can be used as an “order parameter” to identify the transition to the deconfinement region. Note, however, that the increase in d_G of about ~ 1.2 is smaller than that observed increase for the inverse of the electric (longitudinal) gluon propagator at zero momentum, almost a factor of ~ 3 , when crossing T_c . Furthermore, note that our results are similar to previous results using quenched ensembles with smaller lattice volumes [11]. However, our results suggest a stronger transition at T_c .

Temp. (MeV)	$L_s^3 \times L_t$	β	a (fm)	$L_s a$ (fm)
270.1	$72^3 \times 8$	6.058	0.09132	6.58
271.0	$72^3 \times 8$	6.060	0.09101	6.55
271.5	$72^3 \times 8$	6.061	0.09086	6.54
271.9	$72^3 \times 8$	6.062	0.09071	6.53
272.4	$72^3 \times 8$	6.063	0.09055	6.52
273.8	$72^3 \times 8$	6.066	0.09010	6.49

TABLE II: The lattice setup. The physical scale was defined from the string tension. The values of β were adjusted such that $L_s a \simeq 6.5 - 6.6$ fm.

IV. GHOST PROPAGATOR AND CENTER SYMMETRY

The generating functional of pure Yang-Mills theory on the lattice is invariant under center symmetry. In the phase where gluons are deconfined this symmetry is spontaneously broken. The breaking of the center symmetry can be identified by studying the dynamics of the configurations associated with different phases of the Polyakov loop.

For the gluon propagator the effects associated with center symmetry, temperature and the breaking of the center symmetry were studied in [23]. There, after separating the gauge configurations into different Z_3 sectors according to the phase of the Polyakov loop, the gluon propagator was computed in each of the sectors. It turns out that for temperatures below T_c the gluon propagator is blind to the phase of the Polyakov loop. However, for temperatures above T_c , i.e. for temperatures above the deconfinement temperature, the gluon propagator is no longer the same in all the sectors. Indeed, for $T > T_c$, the longitudinal (transverse) gluon propagator for the configurations that return a vanishing phase for the Polyakov loop is suppressed (enhanced) relative to the configurations where the phase of the Polyakov loop is $\pm 2\pi/3$. This difference is an indication of the spontaneous breaking of the center symmetry that occurs at high temperatures. Moreover, the difference between the infrared gluon propagator associated with the Z_3 sectors can be used as an “order parameter” to describe the confinement-to-deconfinement transition. We now aim to investigate how the different dynamics, for temperatures below and above T_c , translate into the ghost propagator.

In order to investigate center symmetry we consider the subset of configurations studied in [23] that are described in Tab. II. In [23] and references therein, the reader can find the details about the characteristics of the gauge ensembles. Note that the lattices are, in principle, sufficiently fine ($a \sim 0.1$ fm) and the physical volumes are sufficiently large ($V \sim (6.5 \text{ fm})^4$) such that the finite volume effects are expected to be small [51].

The ghost propagator and the ghost dressing function for temperatures near T_c and for the various sectors defined according to the phase of the Polyakov loop are

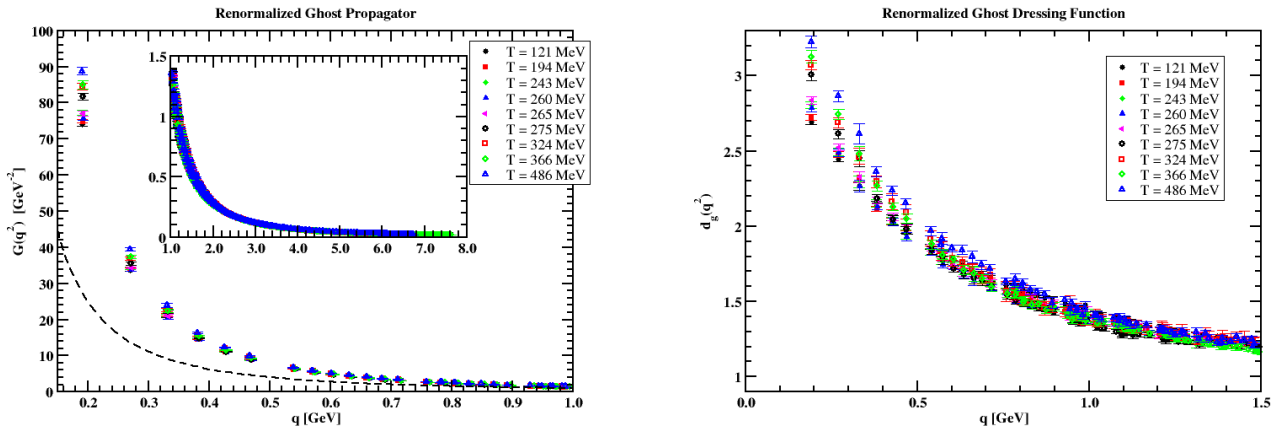


FIG. 1: Landau gauge ghost propagator as a function of the improved momenta q for various temperatures and for the first Matsubara frequency. The left plot shows the propagator for various T , with the dashed line representing the tree level perturbative ghost propagator, while the right plot reports the ghost dressing function.

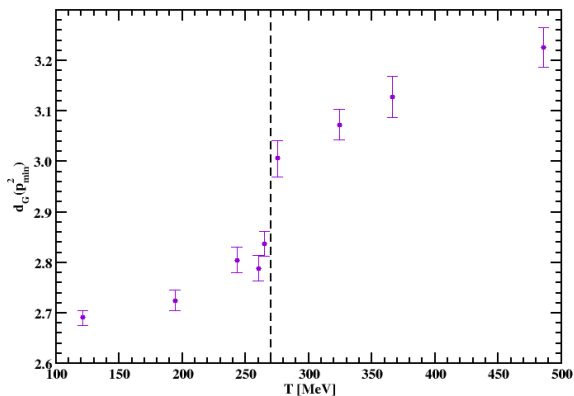


FIG. 2: Landau gauge ghost dressing function at the lowest available momenta $q \sim 0.19$ GeV as a function of T .

reported in Fig. 3. As can be seen, for the smallest temperatures the ghost propagator does not depend on the phase of the Polyakov loop, while for the higher temperatures the ghost propagator for the zero sector is enhanced relative to the propagators associated with the sectors whose Polyakov loop phase is $\pm 2\pi/3$. Note, however, that the propagators associated with a $\pm 2\pi/3$ phase are indistinguishable. As seen in [23], the behavior observed for the ghost propagator follows that observed for the magnetic (transverse) form factor of the gluon propagator, as for the electric (longitudinal) form factor the sector 0 is suppressed relative to the other two sectors that, once more, are indistinguishable.

For completeness in Fig. 4 we report, for each of the

Z_3 sectors, the ghost propagator at the smallest non-zero momentum $q \sim 192$ MeV accessed in our simulations. The Fig. shows that for the smaller temperatures the various propagators are compatible, within two standard deviations, while at the higher temperatures there is a clear separation between the data of the various propagators. Note that the 2σ separation for $T < T_c$ can be due to Gribov copies effects, something not explored in the current work.

V. SUMMARY AND CONCLUSIONS

In the current work the Landau gauge ghost propagator is studied at finite temperature with lattice simulations for pure Yang Mills SU(3) theory. Moreover, its relation with the breaking of the center symmetry is also addressed by looking at the dependence of the propagator with the phase of the Polyakov loop.

The simulations show an enhancement of the ghost form factor above the critical temperature T_c , previously observed in SU(3) studies on smaller volumes [11], while an early investigation for the SU(2) gauge group concluded in favour of a nearly independent ghost propagator with the temperature [53].

The behavior of the ghost propagator with respect to the center symmetry is also investigated and, similarly as found for the gluon propagator [23], for $T < T_c$ the propagator for the various sectors are indistinguishable, while above T_c the propagators associated with the $\pm 2\pi/3$ sectors are suppressed when compared to the zero sector. Our results support the idea of using the difference of the ghost propagator as an “order parameter” to identify the transition to the deconfined phase.

We aim to extend this study over a wider range of

temperatures and investigate the effect of the quark dynamics, measured through the quark propagator, in each of the various Z_3 sectors using both the quenched approximation and the full QCD [54]. We are also studying the confinement-deconfinement transition in other gauges [56, 57].

Acknowledgements

This work was partly supported by the FCT – Fundação para a Ciência e a Tecnologia, I.P., under

Projects Nos. UIDB/04564/2020, UIDP/04564/2020 and CERN/FIS-COM/0029/2017. P. J. S. acknowledges financial support from FCT (Portugal) under Contract No. CEECIND/00488/2017. The authors acknowledge the Laboratory for Advanced Computing at the University of Coimbra (<http://www.uc.pt/lca>) for providing access to the HPC resources that have contributed to the research within this paper. Access to Navigator was partly supported by the FCT Advanced Computing Project 2021.09759.CPCA.

-
- [1] K. Fukushima and T. Hatsuda, Rept. Prog. Phys. **74**, 014001 (2011) doi:10.1088/0034-4885/74/1/014001 [arXiv:1005.4814 [hep-ph]].
- [2] J. O. Andersen, W. R. Naylor and A. Tranberg, Rev. Mod. Phys. **88**, 025001 (2016) doi:10.1103/RevModPhys.88.025001 [arXiv:1411.7176 [hep-ph]].
- [3] G. Odyniec, Lect. Notes Phys. **999**, 3-29 (2022) doi:10.1007/978-3-030-95491-8_1
- [4] O. Oliveira, P. J. Silva, J. I. Skullerud and A. Sternbeck, Phys. Rev. D **99**, no.9, 094506 (2019) doi:10.1103/PhysRevD.99.094506 [arXiv:1809.02541 [hep-lat]].
- [5] A. Virgili, W. Kamleh and D. Leinweber, [arXiv:2209.14864 [hep-lat]].
- [6] O. Oliveira and P. J. Silva, Eur. Phys. J. C **79**, no.9, 793 (2019) doi:10.1140/epjc/s10052-019-7300-8 [arXiv:1903.00263 [hep-lat]].
- [7] S. Borsanyi *et al.* [Wuppertal-Budapest], JHEP **09**, 073 (2010) doi:10.1007/JHEP09(2010)073 [arXiv:1005.3508 [hep-lat]].
- [8] A. Bazavov, T. Bhattacharya, M. Cheng, C. DeTar, H. T. Ding, S. Gottlieb, R. Gupta, P. Hegde, U. M. Heller and F. Karsch, *et al.* Phys. Rev. D **85**, 054503 (2012) doi:10.1103/PhysRevD.85.054503 [arXiv:1111.1710 [hep-lat]].
- [9] A. Dumitru, Y. Guo, Y. Hidaka, C. P. K. Altes and R. D. Pisarski, Phys. Rev. D **86**, 105017 (2012) doi:10.1103/PhysRevD.86.105017 [arXiv:1205.0137 [hep-ph]].
- [10] A. Maas, J. M. Pawłowski, L. von Smekal and D. Spielmann, Phys. Rev. D **85**, 034037 (2012) doi:10.1103/PhysRevD.85.034037 [arXiv:1110.6340 [hep-lat]].
- [11] R. Aouane, V. G. Bornyakov, E. M. Ilgenfritz, V. K. Mitrjushkin, M. Müller-Preussker and A. Sternbeck, Phys. Rev. D **85**, 034501 (2012) doi:10.1103/PhysRevD.85.034501 [arXiv:1108.1735 [hep-lat]].
- [12] V. G. Bornyakov and V. K. Mitrjushkin, Int. J. Mod. Phys. A **27**, 1250050 (2012) doi:10.1142/S0217751X12500509 [arXiv:1103.0442 [hep-lat]].
- [13] A. Maas, Phys. Rept. **524**, 203-300 (2013) doi:10.1016/j.physrep.2012.11.002 [arXiv:1106.3942 [hep-ph]].
- [14] R. Aouane, F. Burger, E. M. Ilgenfritz, M. Müller-Preussker and A. Sternbeck, Phys. Rev. D **87**, no.11, 114502 (2013) doi:10.1103/PhysRevD.87.114502 [arXiv:1212.1102 [hep-lat]].
- [15] P. J. Silva, O. Oliveira, P. Bicudo and N. Cardoso, Phys. Rev. D **89**, no.7, 074503 (2014) doi:10.1103/PhysRevD.89.074503 [arXiv:1310.5629 [hep-lat]].
- [16] A. F. Falcão, O. Oliveira and P. J. Silva, Phys. Rev. D **102**, no.11, 114518 (2020) doi:10.1103/PhysRevD.102.114518 [arXiv:2008.02614 [hep-lat]].
- [17] F. Siringo and G. Comitini, Phys. Rev. D **103**, no.7, 074014 (2021) doi:10.1103/PhysRevD.103.074014 [arXiv:2101.08341 [hep-th]].
- [18] D. M. van Egmond and U. Reinosa, Phys. Rev. D **106**, no.7, 074005 (2022) doi:10.1103/PhysRevD.106.074005 [arXiv:2206.03841 [hep-ph]].
- [19] J. M. Cornwall, Mod. Phys. Lett. A **28**, 1330035 (2013) doi:10.1142/S0217732313300358 [arXiv:1310.7897 [hep-ph]].
- [20] S. W. Li, P. Lowdon, O. Oliveira and P. J. Silva, Phys. Lett. B **803**, 135329 (2020) doi:10.1016/j.physletb.2020.135329 [arXiv:1907.10073 [hep-th]].
- [21] O. Oliveira, L. C. Loveridge and P. J. Silva, EPJ Web Conf. **274**, 02004 (2022) doi:10.1051/epjconf/202227402004 [arXiv:2211.12593 [hep-lat]].
- [22] J. I. Kapusta and C. Gale, Cambridge University Press, 2011, ISBN 978-0-521-17322-3, 978-0-521-82082-0, 978-0-511-22280-1 doi:10.1017/CBO9780511535130
- [23] P. J. Silva and O. Oliveira, Phys. Rev. D **93**, no.11, 114509 (2016) doi:10.1103/PhysRevD.93.114509 [arXiv:1601.01594 [hep-lat]].
- [24] P. M. Lo, B. Friman, O. Kaczmarek, K. Redlich and C. Sasaki, Phys. Rev. D **88**, no.1, 014506 (2013) doi:10.1103/PhysRevD.88.014506 [arXiv:1306.5094 [hep-lat]].
- [25] A. Cucchieri, Nucl. Phys. B **508**, 353-370 (1997) doi:10.1016/S0550-3213(97)00629-9 [arXiv:hep-lat/9705005 [hep-lat]].
- [26] P. J. Silva and O. Oliveira, PoS LATTICE2007, 333 (2007) doi:10.22323/1.042.0333 [arXiv:0710.0669 [hep-lat]].
- [27] P. J. Silva and O. Oliveira, PoS LATTICE2010, 287

- (2010) doi:10.22323/1.105.0287 [arXiv:1011.0483 [hep-lat]].
- [28] P. J. Silva and O. Oliveira, Nucl. Phys. B **690**, 177-198 (2004) doi:10.1016/j.nuclphysb.2004.04.020 [arXiv:hep-lat/0403026 [hep-lat]].
- [29] A. Sternbeck and M. Müller-Preussker, Phys. Lett. B **726**, 396-403 (2013) doi:10.1016/j.physletb.2013.08.017 [arXiv:1211.3057 [hep-lat]].
- [30] R. Kaiser and O. Philipsen, PoS **LATTICE2022**, 175 (2023) doi:10.22323/1.430.0175 [arXiv:2212.14461 [hep-lat]].
- [31] O. Oliveira, V. Paiva and P. Silva, EPJ Web Conf. **274**, 05008 (2022) doi:10.1051/epjconf/202227405008 [arXiv:2301.01229 [hep-lat]].
- [32] H. Suman and K. Schilling, Phys. Lett. B **373**, 314-318 (1996) doi:10.1016/0370-2693(96)00162-1 [arXiv:hep-lat/9512003 [hep-lat]].
- [33] D. B. Leinweber *et al.* [UKQCD], Phys. Rev. D **60**, 094507 (1999) [erratum: Phys. Rev. D **61**, 079901 (2000)] doi:10.1103/PhysRevD.60.094507 [arXiv:hep-lat/9811027 [hep-lat]].
- [34] I. Montvay and G. Munster, Cambridge University Press, 1997, ISBN 978-0-521-59917-7, 978-0-511-87919-7 doi:10.1017/CBO9780511470783
- [35] D. Becirevic, P. Boucaud, J. P. Leroy, J. Micheli, O. Pene, J. Rodriguez-Quintero and C. Roiesnel, Phys. Rev. D **60**, 094509 (1999) doi:10.1103/PhysRevD.60.094509 [arXiv:hep-ph/9903364 [hep-ph]].
- [36] F. de Soto and C. Roiesnel, JHEP **09**, 007 (2007) doi:10.1088/1126-6708/2007/09/007 [arXiv:0705.3523 [hep-lat]].
- [37] M. Vujanovic and T. Mendes, Phys. Rev. D **99**, no.3, 034501 (2019) doi:10.1103/PhysRevD.99.034501 [arXiv:1807.03673 [hep-lat]].
- [38] G. T. R. Catumba, O. Oliveira and P. J. Silva, Phys. Rev. D **103**, no.7, 074501 (2021) doi:10.1103/PhysRevD.103.074501 [arXiv:2101.04978 [hep-lat]].
- [39] A. Cucchieri and T. Mendes, PoS **LATTICE2007**, 297 (2007) doi:10.22323/1.042.0297 [arXiv:0710.0412 [hep-lat]].
- [40] A. Cucchieri, T. Mendes, O. Oliveira and P. J. Silva, Phys. Rev. D **76**, 114507 (2007) doi:10.1103/PhysRevD.76.114507 [arXiv:0705.3367 [hep-lat]].
- [41] I. L. Bogolubsky, E. M. Ilgenfritz, M. Muller-Preussker and A. Sternbeck, Phys. Lett. B **676**, 69-73 (2009) doi:10.1016/j.physletb.2009.04.076 [arXiv:0901.0736 [hep-lat]].
- [42] E. M. Ilgenfritz, C. Menz, M. Muller-Preussker, A. Schiller and A. Sternbeck, Phys. Rev. D **83**, 054506 (2011) doi:10.1103/PhysRevD.83.054506 [arXiv:1010.5120 [hep-lat]].
- [43] A. G. Duarte, O. Oliveira and P. J. Silva, Phys. Rev. D **94**, no.1, 014502 (2016) doi:10.1103/PhysRevD.94.014502 [arXiv:1605.00594 [hep-lat]].
- [44] D. Dudal, O. Oliveira, M. Roelfs and P. Silva, Nucl. Phys. B **952**, 114912 (2020) doi:10.1016/j.nuclphysb.2019.114912 [arXiv:1901.05348 [hep-lat]].
- [45] D. Boito, A. Cucchieri, C. Y. London and T. Mendes, JHEP **02**, 144 (2023) doi:10.1007/JHEP02(2023)144 [arXiv:2210.10490 [hep-lat]].
- [46] A. G. Duarte, O. Oliveira and P. J. Silva, Phys. Rev. D **94**, no.7, 074502 (2016) doi:10.1103/PhysRevD.94.074502 [arXiv:1607.03831 [hep-lat]].
- [47] Y. Iwasaki, K. Kanaya, T. Yoshie, T. Hoshino, T. Shirakawa, Y. Oyanagi, S. Ichii and T. Kawai, Phys. Rev. D **46**, 4657-4667 (1992) doi:10.1103/PhysRevD.46.4657
- [48] G. Boyd, J. Engels, F. Karsch, E. Laermann, C. Legeland, M. Lutgemeier and B. Petersson, Nucl. Phys. B **469**, 419-444 (1996) doi:10.1016/0550-3213(96)00170-8 [arXiv:hep-lat/9602007 [hep-lat]].
- [49] B. Lucini and M. Teper, JHEP **06**, 050 (2001) doi:10.1088/1126-6708/2001/06/050 [arXiv:hep-lat/0103027 [hep-lat]].
- [50] A. Maas, J. M. Pawłowski, L. von Smekal and D. Spielmann, Phys. Rev. D **85**, 034037 (2012) doi:10.1103/PhysRevD.85.034037 [arXiv:1110.6340 [hep-lat]].
- [51] O. Oliveira and P. J. Silva, Phys. Rev. D **86**, 114513 (2012) doi:10.1103/PhysRevD.86.114513 [arXiv:1207.3029 [hep-lat]].
- [52] R. G. Edwards *et al.* [SciDAC, LHPC and UKQCD], Nucl. Phys. B Proc. Suppl. **140**, 832 (2005) doi:10.1016/j.nuclphysbps.2004.11.254 [arXiv:heplat/0409003 [hep-lat]].
- [53] A. Cucchieri, A. Maas and T. Mendes, Phys. Rev. D **75**, 076003 (2007) doi:10.1103/PhysRevD.75.076003 [arXiv:hep-lat/0702022 [hep-lat]].
- [54] P. J. Silva and O. Oliveira, PoS **LATTICE2019**, 047 (2020) doi:10.22323/1.363.0047 [arXiv:1912.13061 [hep-lat]].
- [55] M. Pippig, SIAM J. Sci. Comput. **35**, C213 (2013)
- [56] D. M. van Egmond and U. Reinosa, [arXiv:2304.00756 [hep-th]].
- [57] D. M. van Egmond, U. Reinosa, O. Oliveira, P. J. Silva, *in preparation*

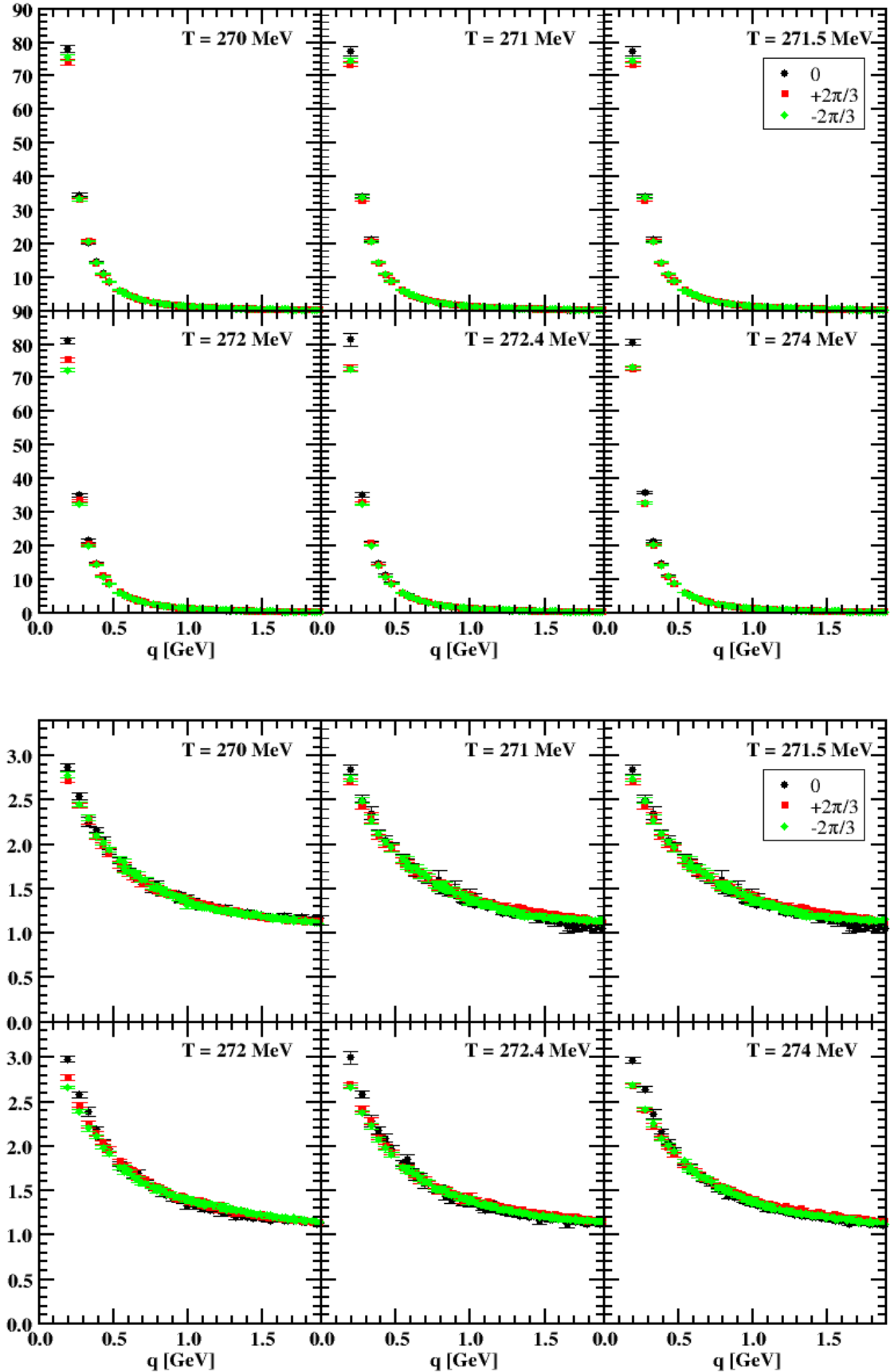


FIG. 3: Renormalized ghost propagator (top) and ghost dressing function (bottom) near T_c and for each of the Z_3 sectors.

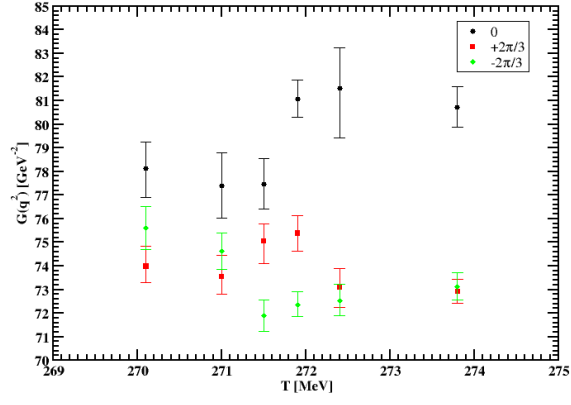


FIG. 4: Renormalized ghost propagator near T_c , at the smallest nonzero momentum $q = 0.19$ GeV and for each of the Z_3 sectors.